JOURNAL OF Applied Polymer SCIENCE

Special Issue: Bio-based Packaging

Guest Editors: José M. Lagarón, Amparo López-Rubio, and María José Fabra
Institute of Agrochemistry and Food Technology of the Spanish Council for Scientific Research

EDITORIAL

REVIEWS

RESEARCH ARTICLES

JOURNAL OF Applied Polymer SCIENCE

Special Issue: Bio-based Packaging

Guest Editors: José M. Lagarón, Amparo López-Rubio, and María José Fabra
Institute of Agrochemistry and Food Technology of the Spanish Council for Scientific Research

Impact of fermentation residues on the thermal, structural, and rheological properties of polyhydroxy(butyrate-*co*-valerate) produced from cheese whey and olive oil mill wastewater
L. Hilliou, D. Machado, C. S. S. Oliveira, A. R. Gouveia, M. A. M. Reis, S. Campanari, M. Villano and M. Majone, *J. Appl. Polym. Sci.* 2015, DOI: 10.1002/app.42818

Synergistic effect of lactic acid oligomers and laminar graphene sheets on the barrier properties of polylactide nanocomposites obtained by the in situ polymerization pre-incorporation method
J. Ambrosio-Martín, A. López-Rubio, M. J. Fabra, M. A. López-Manchado, A. Sorrentino, G. Gorrasi and J. M. Lagarón, *J. Appl. Polym. Sci.* 2015, DOI: 10.1002/app.42661

Antibacterial poly(lactic acid) (PLA) films grafted with electrospun PLA/allyl isothiocyanate fibers for food packaging
H. H. Kara, F. Xiao, M. Sarker, T. Z. Jin, A. M. M. Sousa, C.-K. Liu, P. M. Tomasula and L. Liu, *J. Appl. Polym. Sci.* 2015, DOI: 10.1002/app.42475

Poly(L-lactide)/ZnO nanocomposites as efficient UV-shielding coatings for packaging applications
E. Lizundia, L. Ruiz-Rubio, J. L. Vilas and L. M. León, *J. Appl. Polym. Sci.* 2015, DOI: 10.1002/app.42426

Effect of electron beam irradiation on the properties of polylactic acid/montmorillonite nanocomposites for food packaging applications
M. Salvatore, A. Marra, D. Duraccio, S. Shayanfar, S. D. Pillai, S. Cimmino and C. Silvestre, *J. Appl. Polym. Sci.* 2015, DOI: 10.1002/app.42219

Preparation and characterization of linear and star-shaped poly L-lactide blends
M. B. Khajeheian and A. Rosling, *J. Appl. Polym. Sci.* 2015, DOI: 10.1002/app.42231

Mechanical properties of biodegradable polylactide/poly(ether-block-amide)/thermoplastic starch blends: Effect of the crosslinking of starch
L. Zhou, G. Zhao and W. Jiang, *J. Appl. Polym. Sci.* 2015, DOI: 10.1002/app.42297

Interaction and quantification of thymol in active PLA-based materials containing natural fibers
I. S. M. A. Tawakkal, M. J. Cran and S. W. Bigger, *J. Appl. Polym. Sci.* 2015, DOI: 10.1002/app.42160

Graphene-modified poly(lactic acid) for packaging: Material formulation, processing, and performance
M. Barletta, M. Puopolo, V. Tagliaferri and S. Vesco, *J. Appl. Polym. Sci.* 2015, DOI: 10.1002/app.42252

Edible films based on chia flour: Development and characterization
M. Dick, C. H. Pagno, T. M. H. Costa, A. Gomaa, M. Subirade, A. De O. Rios and S. H. Flóres, *J. Appl. Polym. Sci.* 2015, DOI: 10.1002/app.42455

Influence of citric acid on the properties and stability of starch-polycaprolactone based films
R. Ortega-Toro, S. Collazo-Bigliardi, P. Talens and A. Chiralt, *J. Appl. Polym. Sci.* 2015, DOI: 10.1002/app.42220

Bionanocomposites based on polysaccharides and fibrous clays for packaging applications
A. C. S. Alcântara, M. Darder, P. Aranda, A. Ayral and E. Ruiz-Hitzky, *J. Appl. Polym. Sci.* 2015, DOI: 10.1002/app.42362

Hybrid carrageenan-based formulations for edible film preparation: Benchmarking with kappa carrageenan
F. D. S. Larotonda, M. D. Torres, M. P. Gonçalves, A. M. Sereno and L. Hilliou, *J. Appl. Polym. Sci.* 2015, DOI: 10.1002/app.42263

JOURNAL OF Applied Polymer SCIENCE

Special Issue: Bio-based Packaging

Guest Editors: José M. Lagarón, Amparo López-Rubio, and María José Fabra
Institute of Agrochemistry and Food Technology of the Spanish Council for Scientific Research

Structural and mechanical properties of clay nanocomposite foams based on cellulose for the food packaging industry
S. Ahmadzadeh, J. Keramat, A. Nasirpour, N. Hamdami, T. Behzad, L. Aranda, M. Vilasi and S. Desobry, *J. Appl. Polym. Sci.* 2015, DOI: 10.1002/app.42079

Mechanically strong nanocomposite films based on highly filled carboxymethyl cellulose with graphene oxide
M. El Achaby, N. El Miri, A. Snik, M. Zahouily, K. Abdelouahdi, A. Fihri, A. Barakat and A. Solhy, *J. Appl. Polym. Sci.* 2015, DOI: 10.1002/app.42356

Production and characterization of microfibrillated cellulose-reinforced thermoplastic starch composites
L. Lendvai, J. Karger-Kocsis, Á. Kmetty and S. X. Drakopoulos, *J. Appl. Polym. Sci.* 2015, DOI: 10.1002/app.42397

Development of bioplastics based on agricultural side-stream products: Film extrusion of *Crambe abyssinica*/wheat gluten blends for packaging purposes
H. Rasel, T. Johansson, M. Gällstedt, W. Newson, E. Johansson and M. Hedenqvist, *J. Appl. Polym. Sci.* 2015, DOI: 10.1002/app.42442

Influence of plasticizers on the mechanical and barrier properties of cast biopolymer films
V. Jost and C. Stramm, *J. Appl. Polym. Sci.* 2015, DOI: 10.1002/app.42513

The effect of oxidized ferulic acid on physicochemical properties of bitter vetch (*Vicia ervilia*) protein-based films
A. Arabestani, M. Kadivar, M. Shahedi, S. A. H. Goli and R. Porta, *J. Appl. Polym. Sci.* 2015, DOI: 10.1002/app.42894

Effect of hydrochloric acid on the properties of biodegradable packaging materials of carboxymethylcellulose/poly(vinyl alcohol) blends
M. D. H. Rashid, M. D. S. Rahaman, S. E. Kabir and M. A. Khan, *J. Appl. Polym. Sci.* 2015, DOI: 10.1002/app.42870

Journal of Applied Polymer Science

Graphene-modified poly(lactic acid) for packaging: Material formulation, processing and performance

Massimiliano Barletta,[1] Michela Puopolo,[2] Vincenzo Tagliaferri,[1] Silvia Vesco[1]

[1]Dipartimento di Ingegneria dell'Impresa, Università degli Studi di Roma Tor Vergata, Via del Politecnico, 1 – 00133 Roma, Italy

[2]Dipartimento di Ingegneria Meccanica ed Aerospaziale, Sapienza Università degli Studi di Roma, Via Eudossiana, 18 – 00184 Roma, Italy

Correspondence to: M. Barletta (E-mail: barletta@ing.uniroma2.it)

ABSTRACT: Manufacturing of plastics by compostable polymers is of crucial relevance to limit the environmental impact and reduce oil consumption. Performance of compostable polymers is often mediocre, although they could be improved by physical and chemical routes. In this work, Poly(Lactic Acid) (PLA) is modified for improved performance by two different routes: (1) by physically dispersing Graphene Nano-Platelets (GNP) in the organic matrix; (2) by the physical dispersion and covalent bonding of PLA and Amino-Functionalized Nano-Silica (A-fSiO_2). Functionalization of the PLAs after compounding and pelletizing was assessed by combined Fourier Transform Infrared (FT-IR). In addition, thermal analysis was performed by Differential Scanning Calorimetry (DSC). Mechanical response was evaluated on compression molded flat slabs of the modified PLAs by Pencil and progressive and constant load scratch tests. Chemical endurance was evaluated on compression molded flat slabs of the modified PLAs by dipping in aggressive acidic, basic, and saline environments. Finally, the modified PLAs were successfully injection molded to manufacture high performance coffee capsules, whose thermal stability and suitability to coffee brewing were demonstrated. © 2015 Wiley Periodicals, Inc. J. Appl. Polym. Sci. **2016**, *133*, 42252.

KEYWORDS: biopolymers and renewable polymers; manufacturing; packaging; synthesis and processing

Received 16 January 2015; accepted 19 March 2015

DOI: 10.1002/app.42252

INTRODUCTION

Manufacturing of plastics relies on oil-derived products. In 2012, 32 million tons were the amount of plastics to be dismissed. About 5% of plastics were released in the environment without any further treatments, this being the source of severe environmental impacts. Compostable and biodegradable polymers are of major interest, as they can mitigate the environmental burden. They degrade spontaneously when exposed to light, moisture or bacteria, rely on natural resource, and not on oil-derivatives. In contrast, compostable and biodegradable polymers feature limited thermal and mechanical properties, especially in relation to their high manufacturing cost. Among compostable polymers, neat PLA resin features good elastic modulus and tensile strength, not far from petroleum-based polymers. Nonetheless, PLA is usually rather brittle, featuring limited thermal resistance, toughness, and resiliency. Neat PLA resin is thus improved by compounding PLA through the incorporation of additional materials, like other resins (blending process), mineral fillers, and a large variety of additives (nucleating agents, filler dispersants, bonding agents, impact modifiers, lubricants, melt strength enhancers, etc.) as reported in Refs. 1–3. The dispersion of nano-fillers, including layered silicates, carbon nanotubes, hydroxyapatite, layered titanate, and aluminium hydroxide, to achieve performant PLA nanocomposites is highly explored, despite the growing concerns related to safety issues. Nano-fillers could migrate and, being ingested or inhaled, become significantly dangerous for human health. Other routes are however promising to improve the properties of PLA polymers: (1) reinforcement of the organic matrix with compatible micro-sized mineral fillers featuring high specific surface, (2) chemical bonding of mineral fillers and PLA by intermediate organo-silane or functionalized carbonaceous materials, (3) blending of PLAs with low amount of performant polymers and appropriate additives, (4) fine-tuning of crystallization response in PLA by the addition of nucleating agents, and (5) careful control of the temperature variations during melt processing, which can drive towards the manufacturing of high performance PLAs, compliant with the stringent specifications of the market.

In this respect, compounding of PLAs with other materials was the subject of several investigations. Oksman *et al.*[4] investigated the mechanical properties of PLA composites reinforced with

microcrystalline cellulose, wood flour, and wood pulp. Huda *et al.*[5] reported that the tensile strength for PLA-flax fiber composites is about 50% better than PP-flax composites, currently used in the manufacturing of several automotive panels. Shibata *et al.*[6] evaluated the mechanical and thermo-physical properties of PLA composites reinforced with chopped glass fiber or recycled newspaper cellulose fiber. They suggested that cellulose fiber-reinforced PLA composites overcome glass fiber-reinforced PLA composites for either mechanical or thermo-physical properties, being a valuable alternative for the manufacturing of components with limited load bearing. Shibata *et al.* investigated the effect of dispersing abaca fiber (Manila hemp) in many biodegradable polyesters, including PLA. They found improved flexural moduli for poly(butylenes succinate) and polyestercarbonate/PLA blends using C-shaped molds, as the fiber content in the composite could increase. In contrast, for the PLA-abaca fiber composite, a minimal increase in flexural strength was measured, this being ascribable to the intrinsic high flexural strength of neat PLA.[7] However, a full report of the available studies can be found in the review by Russo *et al.*[8] More recently, Barletta *et al.*[9] reinforced PLA polymers by dispersing micro-talc, being this beneficial to the final properties of the compound. In addition, some of the authors showed the effect of bonding organo-silane molecules[10,11] and modified graphene fillers[12] to improve the mechanical response of organic resin when deposited on inorganic and organic substrates.

In the present investigation, PLA is modified for improved performance by two different routes: (1) physically dispersing GNP in the organic matrix; (2) physical dispersion and covalent bonding of PLA and A-fSiO_2. Functionalization of the PLAs after compounding and pelletizing was assessed by FT-IR. In addition, thermal analysis was performed by DSC. Mechanical response was evaluated on compression molded flat slabs of the modified PLAs by Pencil and progressive and constant load scratch tests. Chemical endurance was evaluated on compression molded flat slabs of the modified PLAs by dipping in aggressive acidic, basic, and saline environments. Finally, the modified PLAs were successfully injection molded to manufacture high performance coffee capsules, whose thermal stability and potential suitability to coffee brewing were demonstrated.

EXPERIMENTAL

Materials

PLA was supplied by Nature Works LLC (Minnetonka, Minnesota, USA). The polymer, Ingeo™ Biopolymer 3260 HP, is a low viscosity proprietary PLA, designed for high flow injection molding. It crystallizes during melt processing in appropriate formulations, leading to opaque engineered materials with improved thermal stability. Reagent grade ascorbic acid, isopropyl alcohol, and butyl acetate were supplied by Sigma Aldrich (Milano, Italy). AminoPropyl TriEthoxy Silane (APTES) and Vinyl TriEthoxy Silane (VTEOS) were supplied by Evonik (Evonik, Essen, Germany). GNP were supplied by Nanesa (Arezzo, Italy). GNP fillers were prepared by centrifugation of 25 mg/ml of a GNP suspension. The resulting precipitate was washed and re-suspended in isopropyl alcohol.

APTES functionalized silica particles (A-fSiO_2) were prepared by a sol–gel reaction of APTES and VTEOS. In particular, 7.2 ml of VTOES and 2.6 ml of APTES were dispersed in 50 ml of isopropyl alcohol under magnetic stirring for 90 min. About 0.9 ml of distilled water was then added drop-wise under magnetic stirring for additional 30 min. The reaction products were, then, used without further processing.

Design and Manufacturing of the Engineered Formulations

Engineered formulations involved the PLA polymer, Ingeo™ Biopolymer 3260 HP, and a number of additives: (1) 500 g PLA Ingeo NatureWorks 3260 HP; (2) nucleating agent Irgastab NA 11 (BASF, Ludwigshafen, Germany) (0.2% wt %); (3) microlamellar talc Luzenac HAR (Imerys, Paris, France) (2 μm size, 7.5 wt %); (4) talc dispersant BYK P-4101 (BYK, Wesel, Germany) (1 wt %); (5) silicone lubricant Tegomer PP SI 401 (Evonik, Essen, Germany) (5 wt %); (6) melt strength enhancer Paraloid BPMS-260 (Dow, Midland, Michigan, USA) (3.5 wt %); and (7) impact modifier Paraloid BPS-515 (Dow, Midland, Michigan, USA) (2 wt %). PLA/GNP was achieved by adding to the aforementioned formulation 1 wt % of the carbonaceous fillers. PLA/A-fSiO_2 was achieved by adding to the aforementioned formulation 5 wt % of the amino-modified silica fillers.

All the mentioned constituents cannot be considered toxic for human health or environment in the amount involved in the investigated formulations. However, further and specific analyses should be performed to assess their suitability for food contact, especially at high temperature.

To formulate the modified PLAs, all the raw materials were predried overnight at 60°C and 15 kPa in a vacuum oven (VD series 23, Binder Gmbh, Tuttlingen, Germany). The materials were then extruded in a double screw extruder (Haake Polylab System, Thermo Scientific, Waltham, Massachusetts, USA) setting the screw speed at 123 rpm and the temperature of the sections at 175(inlet)/180/190/200/200/200/190/190/190(outlet)°C. The resulting extruded material was subsequently cooled and pelletized (Haake Fisions PP1 pelletizer POSTEX, Waltham, Massachusetts, USA).

After pelletizing, the pellets were dried again overnight at 60°C and 15 kPa in the vacuum oven before the compression molding. Compression molding (Hydraulic press LP420B, LabTech Engineering Company, Praksa, Muang, Samutprakarn, Thailand) was carried out by setting the temperature of the pressing plates at 190°C, 5 and 6 min the heating and cooling time, 7–7.5 MPa the applied pressure. Compression molding allows manufacturing PLA substrates 150 × 150 mm^2, which were subsequently used for testing purposes.

Finally, the features of the PLA pellets were tested in a preliminary molding test with a two-stage injection molding equipment (Negri Bossi - NB150, Cologno Monzese, Italy) setting the following process parameters: screw speed 150 rpm, temperature of the inlet section of the barrel 180°C, temperature of the outlet section of the barrel 210°C, back pressure 1.5 MPa (first stage), and 5 MPa (second stage). Fill, hold, and cool time were set at 2 s, 2 s, and 30 s, respectively. The mold temperature was set at 60°C. The resulting capsules were tested according to the

regulation ASTM D 648 for the evaluation of the deflection temperature. The load was 0.46 MPa and applied on a flat (0.25 mm thick) copper bar held firmly on the top of the coffee capsules. The deflection temperature was stored when the bar (that is, the in-built capsules) deflected by 0.25 mm. The capsules were also tested in standard coffee brewing equipment to evaluate their potential suitability to coffee brewing.

FT-IR and DSC

To evaluate the chemical and crystalline structures of the PLA and fillers, FT-IR tests were performed. The preparation of the fillers involved the drying in a thermostatic oven (APT. Line ED (E2), Binder, Bohemia, NY, USA) at 60°C of the aforementioned GNP and A-fSiO$_2$ suspensions. After drying, these fillers were subsequently ground with an agatha mortar. After grinding, FT-IR samples were prepared by thoroughly mixing a small amount of each material to be investigated with spectroscopic grade anhydrous KBr. A pressure of 10 tons was applied for 10 min until a clear pellet was obtained for testing. FT-IR was also performed on pelletized and compression mold of the PLA and modified PLAs.

Thermal analysis was performed by DSC (Netzsch, DSC200PC, Selb, Germany). Dynamic scans in nitrogen flux were performed by ambient temperature to 270°C, setting the heating rate at 5°C/min. Tests were performed on the PLA pellets and on the PLAs after melt processing by compression molding.

Polymer Characterization

Chemical endurance of compression molded PLA, PLA/GNP, and PLA/A-fSiO$_2$ was tested in acidic (HCl, 5 wt %), basic (NaOH, 5 wt %), and saline (NaCl, 5 wt %) environment over 300 h of exposure time.

Hardness of the polymers was evaluated using an ASTM Pencil Test method (ASTM D3363). All of the tests were performed at (20 ± 2)°C and 40% R.H. on compression molded PLA, PLA/GNP, and PLA/A-fSiO$_2$.

Progressive load scratch tests were performed on compression molded PLA, PLA/GNP, and PLA/A-fSiO$_2$ by a micro-Combi tester (CSM Instruments, Peseaux, Switzerland) equipped with a conical indenter tip with a radius of 800 μm. The operating conditions of the progressive test mode entailed the application of a normal load that linearly increases from 0 to 30 N along the scratch pattern with a sliding speed of 1 mm min^{-1}. The constant test mode entailed the application of a normal load of 20 N along the scratch pattern with a sliding speed of 0.2, 1, 5, 25, and 100 mm min^{-1}.

The progressive and constant scratch tests involved three consecutive steps that have previously been discussed: (1) the indenter first profiled the surface with a very small load (prescan, 30 mN), storing the original surface profile that was finally subtracted from the loaded scratch scan profile to determine the depth of surface penetration; (2) the indenter, which had been moved back to the starting location, scan-loaded the track length (applying an increasing or constant load), and the normal and tangential forces were contextually recorded; and (3) a post-scan with a very small load (30 mN) recorded the residual profile to obtain an estimation of the magnitude of the residual scratch ditch and the extent of the immediate recovery. With the distance between the indenter and the evaluation unit being measured in terms of the movement of the translation table, the positional values of the load, and penetration could be addressed to the residual deformation at the same position.

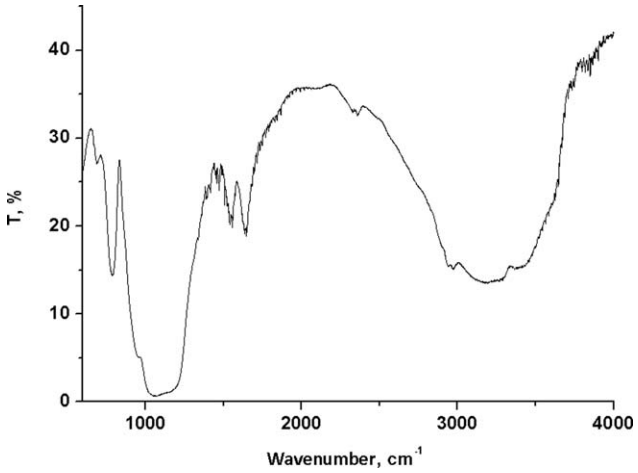

Figure 1. FT-IR spectrum of A-fSiO$_2$.

RESULTS AND DISCUSSION

FT-IR Spectroscopy Analysis

Figure 1 reports the spectra of amino-functionalized SiO$_2$ fillers by the reaction of SiO$_2$ with APTES. A-fSiO$_2$ shows a broad and intense band between 2500 and 4000 cm^{-1}. This band is generated by the overlap of the sharper –NH$_2$ stretching (the amino functionality of APTES), –OH stretching (small residual of –OH group), and C–H stretching bands of the organo-silane. Two sharp additional peaks are found at approximatively 1600 cm^{-1} and 1100 cm^{-1}. A double peak absorption band located at 1600 cm^{-1} is typical of the APTES molecule and attributed to the bending vibrational mode of –NH$_2$ in the lateral side chain. A band at approximately 1100 cm^{-1} is generated by the overlapping of two sharper bands at 1123 and 1037 cm^{-1} and attributed to the vibrations of –Si–O–Si– and –Si–O–C– bonding. In particular, the increase in the 1123 and 1037 cm^{-1} bands and their convolution into a wider single band is ascribable to the chemical structures of amino-fnSiO$_2$, which is prevalently silicic. The presence of the typical APTES absorption bands and of the Si–O–Si bonds should be considered evidence of the grafting reaction between APTES and SiO$_2$.

Figures 2 and 3 reports FT-IR spectra of pelletized and molded PLA without and with modification by the dispersion of GNP and A-fSiO$_2$. The strong peak at approximately 1750 cm^{-1} can be ascribed to the C=O stretching vibrations from carboxylic groups. This peak is very neat and it is substantially constant even when PLA is reinforced with the carbonaceous and silicic fillers. This is the evidence of minor chemical interactions between the organic binder and the fillers, although aminolysis (Figure 4) of the carboxylic groups with the corresponding amino groups is expected to occur. However, aminolysis reaction, if any, occurs very slowly, being substantially absent the stretching band of secondary amide at 3286 cm^{-1} in the FT-IR

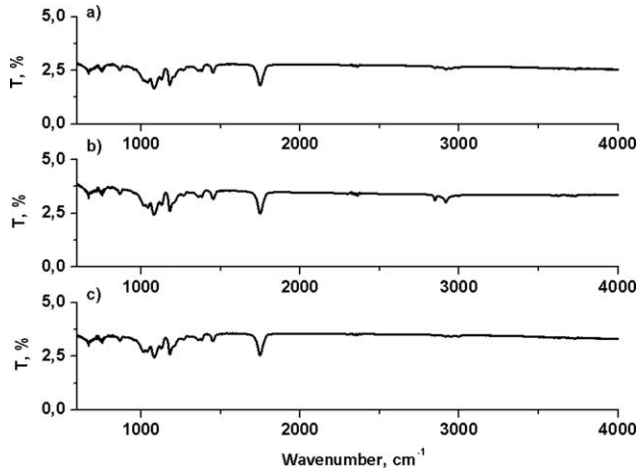

Figure 2. FT-IR spectra of pelletized PLA: (a) PLA; (b) PLA/A-fSiO$_2$; (c) PLA/GNP.

spectra.[13,14] While aminolysis can ensure the tethering of the amino-functionalized silica nano-particles, it is, on the other side, liable of the breaking of the PLA chains. This is supposed to lower the average molecular weight of the resulting composite material and, accordingly, affect the chemical, physical, and mechanical properties.

The resonances due to C–CH$_3$ stretching mode, –CH$_3$ rocking mode, and –CH$_3$ asymmetric bending mode of PLA are found in agreement with Refs. 15–19 at approximately 1080, 1181, and 1454 cm^{-1}, respectively.

FT-IR spectrum of PLA/A-fSiO$_2$ features a band at approximately 2800 cm^{-1}, this being the residuals of the intense band of the A-fSiO$_2$ ascribed to the overlap of the sharper –NH$_2$ stretching (the amino functionality of APTES), –OH stretching (small residual of –OH group), and C–H stretching bands of the organo-silane.

After compression molding process, FT-IR spectra of PLA without and with modification by the dispersion of GNP and A-fSiO$_2$ are substantially unaltered. The progressive disappearance

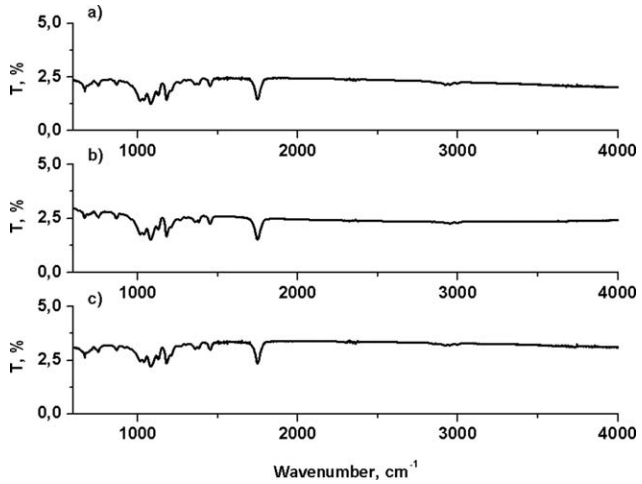

Figure 3. FT-IR spectra of molded PLA: (a) PLA; (b) PLA/A-fSiO$_2$; (c) PLA/GNP.

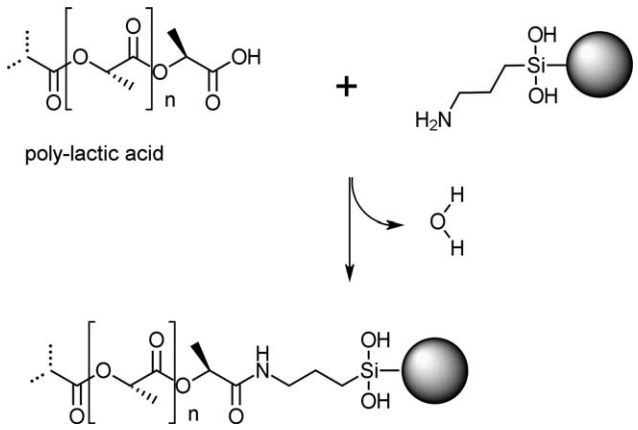

Figure 4. Aminolysis of Poly(Lactic Acid).

of the band of the A-fSiO$_2$ at approximately 2800 cm^{-1} is noted, this being probably attributable to the additional thermal processing of the polymer. Indeed, PLA is known to be extremely susceptible to heat, this being probably the case of the concealing of the band at 2800 cm^{-1}.

Thermal Analysis

DSC analysis showed the thermal transitions of PLA, PLA/GNP, and PLA/A-fSiO$_2$ after pelletizing and melt processing (Figure 5). DSC thermographs performed on the pellets simulate what happens to the polymeric materials during an additional melt processing. In contrast, DSC thermographs performed on the material after compression molding simulate what would happen to the polymeric materials in the case of an additional heating step, they should undergone during their practical applications (for example, the coffee capsules after being shaped by injection molding are re-heated one additional time during coffee brewing before being dismissed). After pelletizing, the glass transition temperature is of approximately 62°C. The glass transition temperature is not influenced by the modifications of PLA by the carbonaceous or functionalized silica particles. The

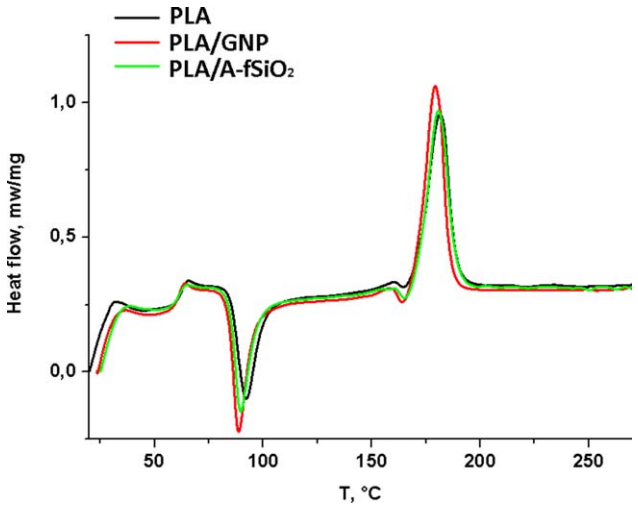

Figure 5. Differential scanning calorimetry of PLA, PLA/GNP, and PLA/A-fSiO$_2$ after pelleting. [Color figure can be viewed in the online issue, which is available at wileyonlinelibrary.com.]

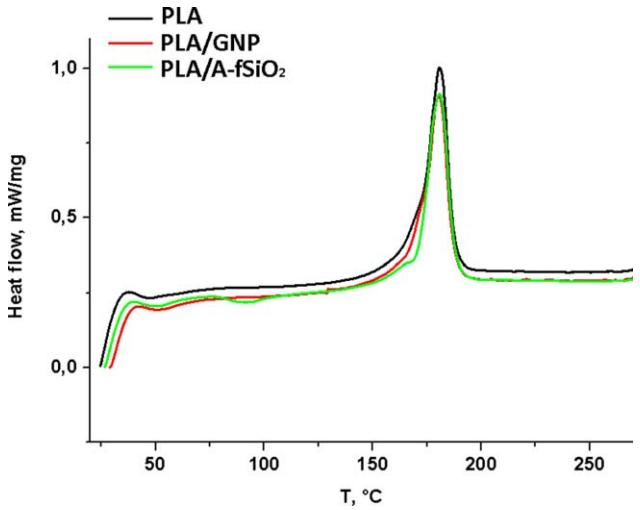

Figure 6. Differential scanning calorimetry of PLA, PLA/GNP, and PLA/A-fSiO$_2$ after molding. [Color figure can be viewed in the online issue, which is available at wileyonlinelibrary.com.]

PLA pellets show sharp crystallization peaks in the range of 90–95°C. Indeed, the polymeric materials exhibit a significant crystallization inside the crucibles during the DSC tests, as it might be observed in the mold, during a compression or injection molding step. The PLA shows the shortest peak and highest crystallization temperature of approximately 94°C. PLA/GNP and PLA/A-fSiO$_2$ exhibit sharpest crystallization peaks and lower crystallization temperatures of approximately 89 and 90°C, respectively. This result can be ascribed to the presence of the particles themselves. They act as nucleating agents, thus promoting the crystallization of the resin. Crystallization occurs earlier (that is, at lower temperature) and the expected degree of crystallization, being related to the extent of the area of the crystallization peaks, is higher for the reinforced PLAs. However, the aforementioned results match data reported in the literature, whereas the relationship between the crystallinity of PLA and the presence of fillers inside the formulation was already known.[20–22] Nonetheless, by comparing the crystallization peaks of PLA/GNP and PLA/A-fSiO$_2$, graphene seems to be more effective in promoting crystallization. The role of graphene and, especially graphene oxide, as nucleating agent was already clarified in Ref. 23. They found a significant increase in melt crystallization rates of PLAs reinforced by graphene oxide, indicating that graphene oxyde (GO) might act as an effective nucleating agent. Similarly, Armentano *et al.*[24] showed a strong relation between GO concentration and PLA crystallization rate, despite high concentration of the reinforcing phase can lead to the onset of defective crystals. The mechanism by which graphene oxide or reduced graphene oxides promotes crystallinity in PLA polymers is still under discussion. However, graphene can be inferred to act similarly. Graphene and graphene-like compounds feature a very high surface to volume ratio, this being extremely beneficial to the formation of first crystallization nuclei and their subsequent growth inside the polymeric material. In this respect, good dispersion of graphene particles inside the polymeric material is of fundamental importance, as crystallization should be favored by the physical presence of the small graphene particles with a high surface ratio rather than to chemical combination or chemical promoted rearrangements of the polymer microstructure.

Melting peaks of the pellets are found at approximately 180°C, with minimum difference arising between the as-is and reinforced polymers. Indeed, the melting peaks are related to the degree of crystallinity of the polymers. As said before, the GNP acts better to promote the crystallization of the PLA, thus determining a higher degree of crystallinity and, concurrently, the release of a high melting enthalpy. In contrast, the PLA alone features the lowest heat of crystallization and, accordingly, the

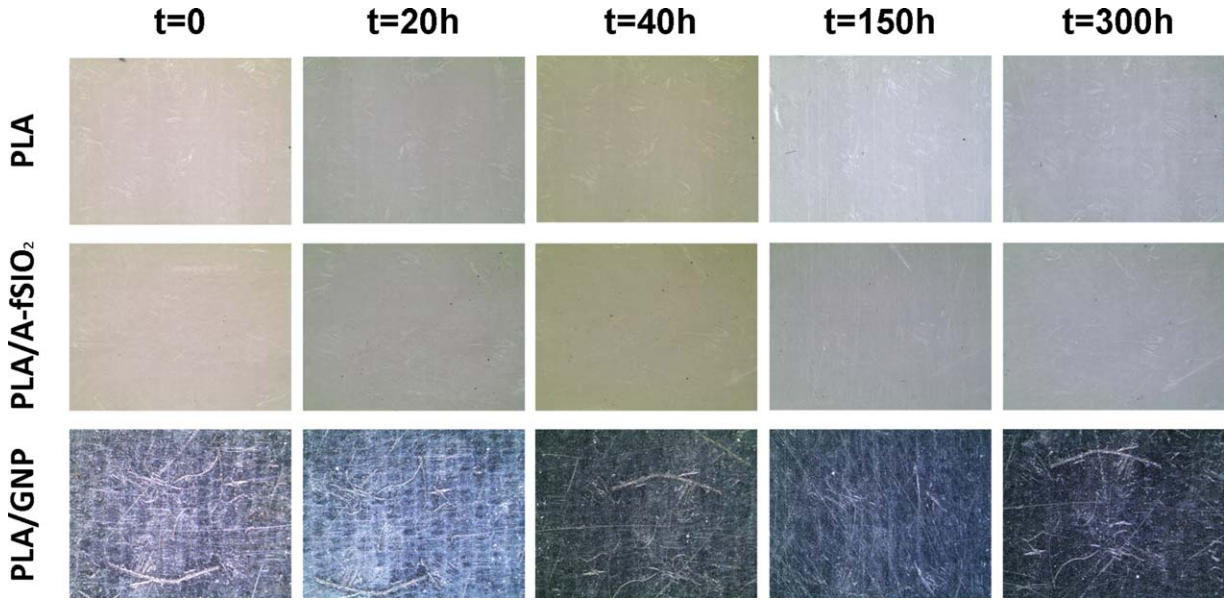

Figure 7. Dipping of molded PLA substrates in acidic environment (HCl, 5 wt %): surface status PLA, PLA/GNP, and PLA/A-fSiO$_2$ after different dipping time. [Color figure can be viewed in the online issue, which is available at wileyonlinelibrary.com.]

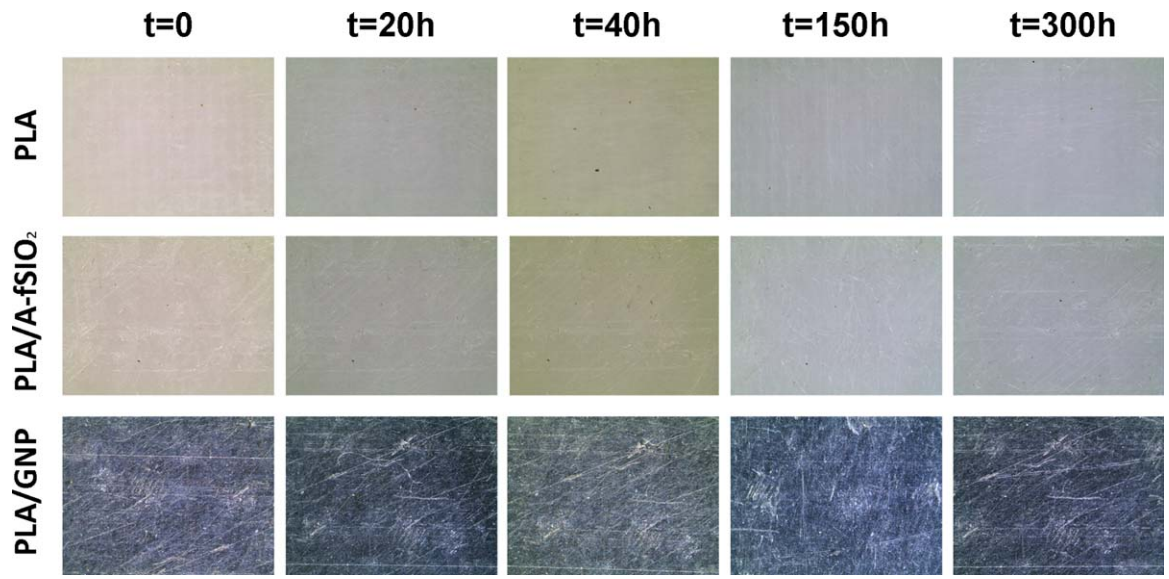

Figure 8. Dipping of PLA substrates in saline environment (NaCl, 5 wt %): surface status PLA, PLA/GNP, and PLA/A-fSiO$_2$ after different dipping time. [Color figure can be viewed in the online issue, which is available at wileyonlinelibrary.com.]

lowest release of enthalpy during the subsequent melting. However, the differences arisen among the polymers in terms of crystallization and melting response are very small.

Figure 6 reports the DSC of PLA and modified PLAs after melt processing (compression molding of the pellets). This time, there are no crystallization peaks. The polymers re-crystalize during the previous extrusion process for the manufacturing of the pellets, as their composition already features the nucleating agents and the fillers, which promote the definitive rearrangement of their structures. Significant heat of crystallization is, therefore, not observed again. A small area is, however, observed in the case of A-fSiO$_2$/PLA, evidence of a very small additional crystallization step.

Melting peaks of the polymers after compression molding are of approximately 180°C. This time, glass transition temperatures cannot be appreciated, thus demonstrating the reduction in the amorphous phase and prevalence of the crystalline phase after melt processing. There is no significant difference among PLA, PLA/GNP, and PLA/A-fSiO$_2$, this being essentially ascribable to the formulations involved during melt processing. As reported in the Experimental section, all the engineered formulations involve a large presence of lamellar talc and other additives (especially, nucleating agents). Together to the specific additive (Irgastab NA 11), the lamellar talc is known to act as effective nucleating agent for PLA resin,[20–22] this overshadowing the role of the fillers. As a result, the melting peaks of the PLA and

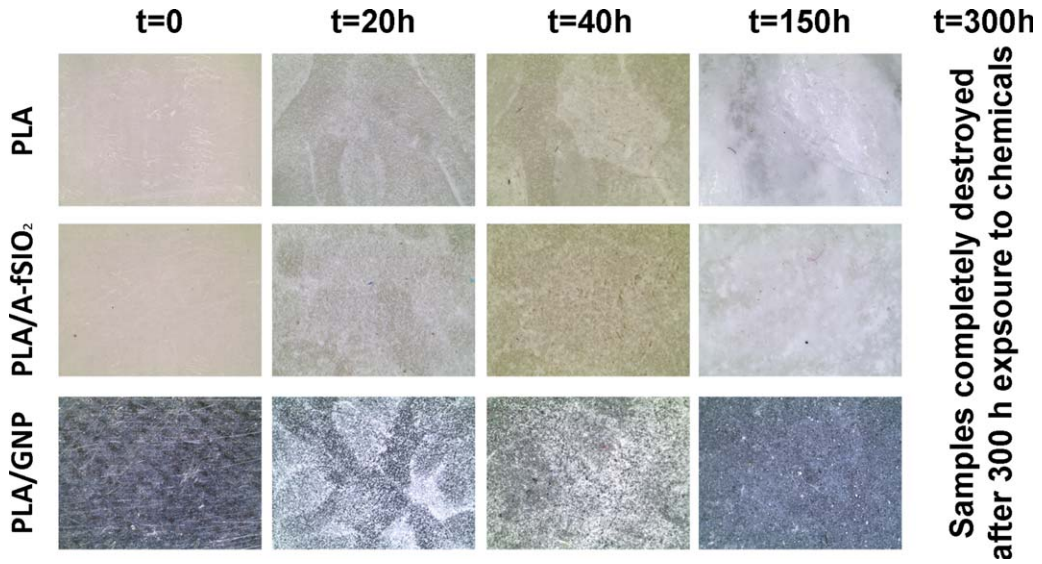

Figure 9. Dipping of PLA substrates in basic environment (NaOH, 5 wt %): surface status PLA, PLA/GNP, and PLA/A-fSiO$_2$ after different dipping time. [Color figure can be viewed in the online issue, which is available at wileyonlinelibrary.com.]

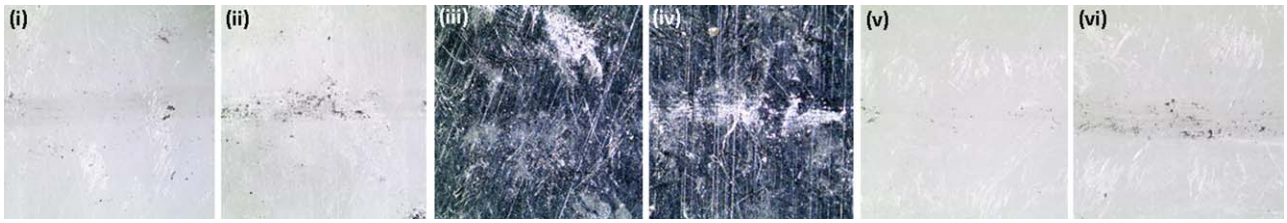

Figure 10. Pencil Test: (i) PLA 3H (pass); (ii) PLA 4H (fail); (iii) PLA/GNP 4H (pass); (iv) PLA/GNP 5H (fail); (v) PLA/A-fSiO$_2$ 4H (pass); (vi) PLA/A-fSiO$_2$ 5H (fail).[Color figure can be viewed in the online issue, which is available at wileyonlinelibrary.com.]

modified PLAs are rather similar, with minimum differences arising.

Chemical Endurance

Chemical endurance of PLA and, especially, of reinforced PLA is scarcely investigated. Being a compostable material, PLA is not very often tested for its durability over long time range. Nonetheless, resistance in aggressive environments is a crucial property of PLAs, especially for those which find applications in food packaging or in manufacturing of medical devices and tissue engineering.[25] Under these circumstances, PLAs can come in touch with aggressive environments, which could accelerate degradation process of the resin or, more appropriately, the migration of potentially toxic or harmful species. In food packaging, packaging material comes often in touch with non-neutral or saline environments. Figure 7 shows the evolution over 300 h exposure time in acidic environment (HCl 5 wt %) of compression molded PLA and compression molded PLA/GNP and PLA/A-fSiO$_2$. PLA and modified PLAs show good resistance. The surface of the different PLAs is not impaired during the test. Only a slight change in the color is detectable. In particular, the surface of PLA and PLA/A-fSiO$_2$ becomes more opaque. In addition, the surface morphology becomes progressively coarser (from 150 h exposure time), this being ascribable to the onset of chemical attacks of the aggressive HCl solution. The surface of PLA/GNP undergoes a change in color, which becomes slightly darker. However, there is no evidence of chemical attack of the surface, which is not impaired even after the end of the exposure time (300 h).

The good result of the PLA/GNP can be ascribed to the graphene itself, which is known to be chemically stable and inert.[26,27] PLA and modified compression molded PLA substrates show a worse response to saline environment (Figure 8).

PLA and PLA/A-fSiO$_2$ turns their color very soon (after only 20 h), which becomes progressively more opaque. Increasing the exposure time, their surface becomes first more porous (i.e., onset of pitting) and coarse and later some sub-surface swelling and local bulging (starting from 150 h) can be noted. Exfoliation of the material ultimately occurs, thus severely impairing the substrates. PLA/GNP shows a slightly better response to saline environment. The substrates show some changes in color, while the onset of pitting occurs later (after 40 h). At the end of the test, severe pitting is spread on the substrate surface, but

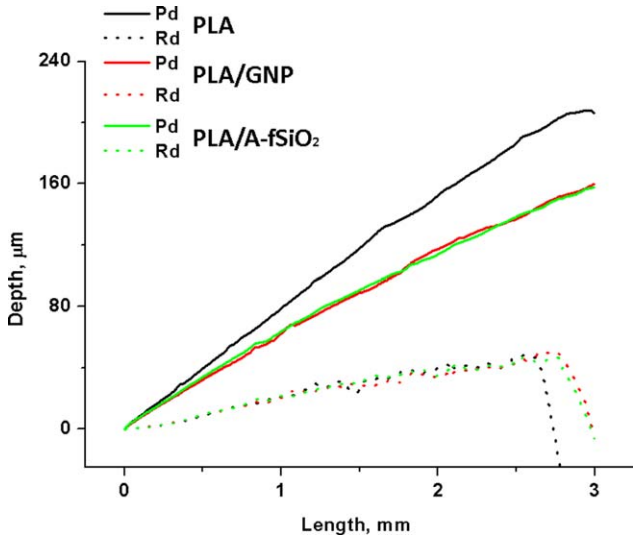

Figure 11. Progressive load scratch tests of molded PLAs: trends of the penetration depth vs sliding distance (length) for PLA, PLA/GNP, and PLA/A-fSiO$_2$. [Color figure can be viewed in the online issue, which is available at wileyonlinelibrary.com.]

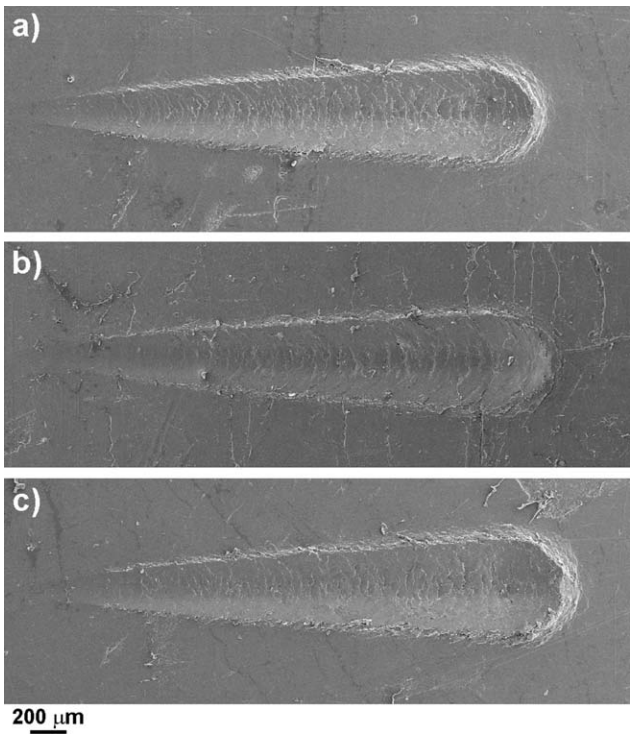

Figure 12. SEM micrographs of the residual scratch patterns after progressive load scratch tests of molded PLAs: (a) as-molded PLA; (b) PLA/A-fSiO$_2$; and (c) PLA/GNP.

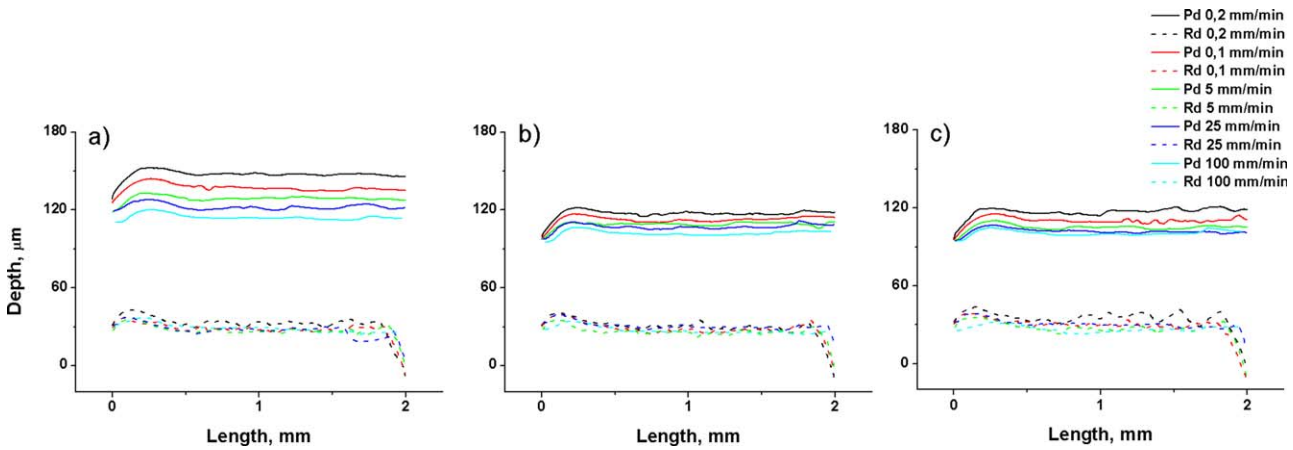

Figure 13. Trends of the penetration depth vs sliding distance (length) after constant load scratch tests of molded PLAs: (a) as-molded PLA; (b) PLA/A-fSiO$_2$; and (c) PLA/GNP. [Color figure can be viewed in the online issue, which is available at wileyonlinelibrary.com.]

no evidence of material exfoliation can be emphasized. Dipping in basic environment (Figure 9) is still more disruptive for all the substrates under investigation. However, PLA/GNP is the most inert substrate to alkaline environment at the end of the test. However, all the substrates exhibit severe damage rather soon, whose onset is clearly visible after just 20 h exposure time. Figure 9 shows some brighter zones, which are the result of the pitting of the substrates surface. These impaired zones tend to grow rather quickly during the test and, after only 40 h exposure time, they involve most of the surface. After 150 h exposure time, all the PLA substrates are significantly impaired, this being the reason of the early termination of the test. However, pitting is more severe on PLA and PLA/A-fSiO$_2$. The better response of PLA/GNP can be inferred to the known inertness of the carbonaceous filler.

Pencil Test

Hardness of molded PLAs is, therefore, tested by Pencil Test. Hardness of PLA is increased by the reinforcement with the graphene and functionalized silica particles. In fact, hardness of the PLA is 3H, while hardness of modified PLAs is 4 H. Figure 10 shows the scratches on the surfaces of the PLA substrates, when tested with two tips with subsequent and increasing hardness.

The carbonaceous and silicic reinforces are able to sustain better the organic PLA matrix to withstand the action of the Pencil tips, with the onset of permanent scratches arising at Pencil Hardness of 4H. In contrast, PLA alone shows sign of permanent scratches arising at Pencil Hardness of 3H.

Scratch Test

Increased stiffness of PLA/GNP and PLA/A-fSiO$_2$ is also confirmed by progressive and constant load scratch tests. In particular, the trends of the penetration tests during progressive load scratch tests show the improved resistance to penetration under load of the modified PLA. PLA show penetration depths much higher whatever the applied load. Modified PLAs show penetration depths of approximately 25–30% less. After the

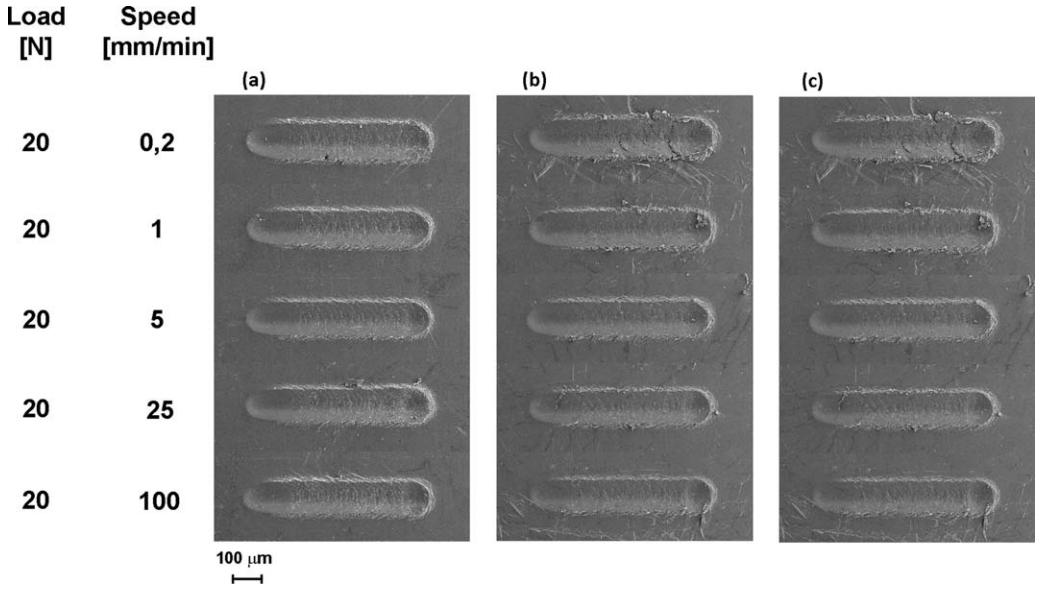

Figure 14. SEM micrographs of the residual scratch patterns after constant load scratch tests of molded PLAs: (a) as-molded PLA; (b) PLA/A-fSiO$_2$; and (c) PLA/GNP.

Figure 15. Coffee capsules: (i) polypropylene; (ii) PLA/GNP; and (iii) PLA/A-fSiO$_2$. [Color figure can be viewed in the online issue, which is available at wileyonlinelibrary.com.]

release of the load, the different PLA substrates behave similarly (Figure 11).

The improved resistance to penetration under load of modified PLAs can be ascribed to the role of the fillers. The fillers feature elastic moduli dramatically higher than PLA binder. As a result, the composite material of the PLA binder with the fillers dispersed inside would feature improved moduli and, accordingly, increased stiffness. In addition, the fillers are physically dispersed in the organic matrix and, in the case of silica filler, it could be bonded to the organic matrix through the amino-functionality. Amino groups can be inferred to combine with the ester groups of PLA by aminolysis as shown in Figure 4.[13,14] This creates a stronger network between matrix and filler, which is able to withstand better the action of the indenter tip during the application of the load. On the other side, GNP features the highest elastic moduli. Therefore, it promotes a significant increase of the stiffness of the PLA/GNP composite, even if it is not designed to chemically combine with the organic matrix. After the load release, the good recover ability of the engineered formulations of the PLA allows similar response in terms of residual depths, without any significant influence of the fillers. Engineered PLA formulations feature an elastic field very wide and comparable to those of more performant oil-derived polymeric material. For this reason, engineered PLA formulations show outstanding recovery in the elastic field, thus explaining the trends of the residual depth in Figure 11 and the lack of any role of the carbonaceous and silica fillers.

Figure 12 shows the SEM images of the residual patterns of the progressive load scratch tests. PLA shows small cracks, which start at very low loads (onset of cracks is at approximately 4.8 N) [Figure 12(a)]. The cracks are)-*shaped* and oriented in the same direction of the advancing indenter according to the mechanism of the conformal cracking.[28] PLA/A-fSiO$_2$ [Figure 12(b)] and PLA/GNP [Figure 12(c)] shows the onset of the aforementioned cracks at higher loads (approximately 7.2 and 7.6 N, for PLA/GNP and PLA/A-fSiO$_2$, respectively), being this the evidence of improved scratch response. Indeed, the better scratch response can be ascribed to the increased stiffness of the reinforced PLA during scratch test. The reinforced materials deform less during the application of the scratch load and, accordingly, exhibit smaller fractures and only after the applications of higher loads.

Figure 12 also shows the presence of pile-up at the sides and ahead the scratch patterns after the progressive load scratch tests. Pile-up is ascribed to the plastic deformation of the polymeric material, which, under the action of the advancing indenter, is pushed away and accumulates around the residual scratch patterns. The presence of the silica and carbonaceous fillers do not influence the extent of the pile-up. This result matches with the trends of residual depths, which are found to be not related to the presence of the fillers inside the polymeric matrix. Pile-up is established on the material after the recovery in the elastic field. As all the investigated PLAs show similar response after the recovery in the elastic field of the polymer, it is reasonable to find similar extents of the pile-up on them after scratch tests.

Figure 13 shows the constant load scratch tests, where the increased stiffness of the PLA/GNP and PLA/A-fSiO$_2$ is confirmed whatever the scratch speed. In addition, molded PLAs feature an apparent increase in the stiffness of the response to the scratch load, when the scratch speed is increased. This result reveals the time dependent scratch response of the molded PLAs, which agrees with similar findings in Refs. 29, 30. The time dependent scratch response of the PLAs is preserved although reprocessing of the PLA pellets by compression molding and their modification by the addition of the fillers and numerous additives in the engineered formulations.

Figure 14 shows the residual scratch patterns of the PLAs after constant load scratch tests. Small cracks by conformal cracking are sparse in the bottom of the residual scratch pattern of PLA and modified PLAs. However, PLAs shows a higher density of larger cracks whatever the sliding speeds.

PLA/GNP and PLA/A-fSiO$_2$ show lower densities of thinner cracks regardless the setting of the sliding speeds. Similarly, pile-up can be noted at the sides and ahead of the residual scratch patterns. In agreement with previous findings, the extent of the pile-up is not related to the specific formulations of the PLAs and, especially, the fillers do not play any significant role.

Manufacturing of the Coffee Capsules

PLA pellets are finally devoted to the manufacturing of prototypal coffee capsules. Figure 15 shows the coffee capsules manufactured by a double-stage injection molding equipment, using commercial polypropylene and the two modified PLAs (PLA/GNP and PLA/A-fSiO$_2$). The coffee capsules manufactured from modified PLA show a good stiffness. When tested for thermal stability, they do not show any deflection up to 120°C, being this temperature suitable for coffee brewing equipments.

The coffee capsules were also tested in automatic coffee brewing machine showing good overall performance, including good attitude to perforation by steel needles during the initial stage of the coffee brewing. This is extremely important, as, softer and ductile materials like polypropylene are rather troublesome to perforate, being subject to large deformations when in contact with the metal needles. This avoids correct perforation of the capsules, compromising the brewing process as well as promoting the early deterioration of the brewing device.

CONCLUSIONS

In the present investigation, PLA is modified for improved physical, chemical, and mechanical performance by two different routes: (1) physically dispersing GNP in the organic matrix; and (2) physical dispersion and covalent bonding of PLA and A-fSiO_2.

Based on the experimental results and theoretical considerations, the following conclusions can be drawn:

- Dispersing nanoparticles inside PLA resin allows improvement in the thermal stability of the compostable polymer as a result of the increased crystallinity and crystallization rate; glass transition temperature disappears in PLA engineered formulations after melt processing and the peak melting points overcome 180°C;
- PLA/GNP improves significantly the chemical inertness of the compostable polymer in acidic, basic, and saline environment over 300 h exposure time;
- Dispersing graphene and silica nanoparticles inside the PLA matrix was found to significantly increase the stiffness of the compostable polymers during scratch tests with the application of both progressive and constant load; similarly, the composites PLA/GNP and PLA/A-fSiO_2 show an increased hardness during Pencil Test;
- PLA/GNP and PLA/A-fSiO_2 exhibit better scratch response, stated by the onset of fractures by conformal cracking at higher load if compared with PLA;
- Constant load scratch tests show viscoelastic response of molded PLA and modified PLAs, which become progressively stiffer at any time faster sliding speeds are set during the scratch tests;
- PLAs show a higher density of larger cracks whatever the sliding speeds. PLA/GNP and PLA/A-fSiO_2 show lower densities of thinner cracks, thus confirming an improved scratch response.

Finally, the modified PLAs were successfully injection molded to manufacture high performance prototypal coffee capsules. The resulting coffee capsules feature high thermal stability (up to 120°C) and are potentially suitable to coffee brewing equipments, especially during perforation by metal needles in the initial stage of coffee brewing.

ACKNOWLEDGMENTS

The authors wish to thank you Prof. Pietro Russo (Researcher at Institute of Chemistry and Polymer Technology, Naples) for the support during the manufacturing of the polymeric materials and, also, for his stimulating insights and suggestions.

REFERENCES

1. Yu, L.; Dean, K.; Li, L. *Prog. Polym. Sci.* **2006**, *31*, 576.
2. Mohanty, A. K.; Misra, M.; Hinrichsen, G. *Macromol. Mater. Eng.* **2000**, *276/277*, 1.
3. Mathew, A. P.; Oksman, K.; Sain, M. *J. Appl. Polym. Sci.* **2005**, *97*, 2014.
4. Oksman, K.; Skrifvars, M.; Selin, J. F. *Compos. Sci. Technol.* **2003**, *63*, 1317.
5. Huda, M. S.; Drzal, L. T.; Mohanty, A. K.; Misra, M. *Compos. Sci. Technol.* **2006**, *66*, 1813.
6. Shibata, M.; Ozawa, K.; Teramoto, N.; Yosomiya, R.; Takeishi, H. *Macromol. Mater. Eng.* **2003**, *288*, 35.
7. Lim, L. T.; Auras, R.; Rubino, M. *Prog. Polym. Sci.* **2008**, *33*, 820.
8. Russo, P.; Acierno, D.; Vignali, A.; Lavorgna, M. *Polym. Compos.* **2014**, *35*, 1093.
9. Barletta, M.; Vesco, S.; Rubino, G.; Puopolo, M.; Venettacci, S. *J. Appl. Polym. Sci.* **2014**, *131*, 40624.
10. Barletta, M.; Pezzola, S.; Puopolo, M.; Tagliaferri, V.; Vesco, S. *Mater. Des.* **2014**, *54*, 924.
11. Barletta, M.; Vesco, S.; Puopolo, M.; Tagliaferri, V. *Mater. Des.* submitted, **2015**
12. Shukla, S. R.; Harad, A. M. *Polym. Degrad. Stab.* **2006**, *91*, 1850.
13. Hoang, C. N.; Dang, Y. H. *Polym. Degrad. Stab.* **2013**, *98*, 697.
14. Li, W.; Xu, Z.; Chen, L.; Shan, M.; Tian, X.; Yang, C.; Lv, H.; Qian, X. *Chem. Eng. J.* **2014**, *237*, 291.
15. Song, W.; Zheng, Z.; Tang, W.; Wang, X. *Polymer* **2007**, *48*, 3658.
16. Yoon, J. T.; Jeong, Y. G.; Lee, S. C.; Min, B. G. *Polym. Adv. Technol.* **2009**, *20*, 631.
17. Amirian, M.; Chakoli, A. N.; Sui, J. H.; Cai, W. *Polym. Bull.* **2012**, *68*, 1747.
18. Olalde, B.; Aizpurua, J. M.; Garcia, A.; Bustero, I.; Obieta, I.; Jurado, M. J. *J. Phys. Chem. C* **2008**, *112*, 10663.
19. Chen, G. X.; Kim, H. S.; Park, B. H.; Yoon, J. S. *J. Phys. Chem. B* **2005**, *109*, 22237.
20. Kolstad, J. J. *J. Appl. Polym. Sci.* **1996**, *62*, 1079.
21. Li, H.; Huneault, M. A. Nucleation and crystallization of PLA. In ANTEC 2007, **2007**, p 2615.
22. Wang, H.; Qiu, Z. *Thermochim. Acta* **2012**, *527*, 40.
23. Chen, H. M.; Zhang, W. B.; Du, X. C.; Yang, J. H.; Zhang, N.; Huang, T.; Wang, Y. *Thermochim. Acta* **2013**, *566*, 57.
24. Armentano, I.; Bitinis, N.; Fortunati, E.; Mattioli, S.; Rescignano, N.; Verdejo, R.; Lopez-Machado, M. A.; Kenny, J. M. *Prog. Polym. Sci.* **2013**, *38*, 1720.
25. Kirkland, N. T.; Schiller, T.; Medhekar, N.; Birbilis, N. *Corros. Sci.* **2012**, *56*, 1.
26. Liu, J.; Hua, L.; Li, S.; Yu, M. *Appl. Surf. Sci.* **2015**, *327*, 241.

27. Shukla, S. R.; Harad, A. M. *Polym. Degrad. Stab.* **2006**, *91*, 1850.
28. Bull, S. J. *Surf. Coat. Technol.* **1991**, *50*, 25.
29. Jardret, V.; Morel, P. *Prog. Org. Coat.* **2003**, *48*, 322.
30. Barletta, M.; Tagliaferri, V.; Gisario, A.; Venettacci, S. *Tribol. Int.* **2013**, *64*, 39.